Angewandte Chemie
Eine Zeitschrift der Gesellschaft Deutscher Chemiker

Supporting Information

69451 Weinheim, Germany

The Fluorenyl Cation**

Paolo Costa, Iris Trosien, Miguel Fernandez-Oliva, Elsa Sanchez-Garcia, and Wolfram Sander**

ange_201411234_sm_miscellaneous_information.pdf

Experimental Section

Materials. All chemicals and solvents were used as received without further purification. Most compounds were purchased from Sigma Aldrich if not noted otherwise. p-Toluenesulfonyl hydrazide was purchased from ABCR and deuterated water (99% D) was purchased from Deutero GmbH.

9-Diazofluorene 5 was synthesized according to a literature procedure starting from 9-Fluorenone.[1] ^{1}H-NMR (200 MHz, DMSO-d_6): δ = 8.09 (d, *J* = 7.4 Hz, 2H, Ar*H*), 7.72 (d, *J* = 7.0 Hz, 2H, Ar*H*), 7.37 (m, 4H, Ar*H*). ^{13}C NMR (50 MHz, DMSO): δ = 132.47, 130.68, 126.43, 124.50, 121.13, 119.80.

9*H*-Fluoren-9-*d*-9-ol-*d* d_2-**4**. Fluorenol **4** was prepared according to a literature procedure[2] by replacing benzophenone with 9-fluorenone. d_2-**4** was synthesized by washing **4** several times with D_2O. ^{1}HNMR (200 MHz, $CDCl_3$) δ 7.63 (m, 4H, Ar*H*), 7.35 (m, 4H, Ar*H*). MS (EI) *m/z* for $C_{13}H_8D_2O$: Calculated: 184 g/mol. Found: 184 $[M]^+$, 166 $[M\text{-}DOD]^+$, 154 $[M\text{-}CDOD]^+$, 77 $[M\text{-}PhCDOD]^+$, 51.$[M\text{-}C_2H_4PhCDOD]^+$

Preparation of low density amorphous ice (LDA). Ultrapure water was degassed in several freeze-thaw cycles. The water partial pressure was controlled by a fine metering valve, and water was co-deposited with **5** in a high vacuum system on top of different substrates (Cu rod, CsI and sapphire windows respectively for EPR, FT-IR and UV-Vis spectroscopy) precooled to 50 K. After deposition, the matrices were cooled to 3 – 5 K.

Matrix isolation spectroscopy. Matrix isolation experiments were performed by standard techniques using Sumitomo Heavy industries two-staged closed-cycle helium cryostats (cooling power 1 W at 4 K) to obtain temperatures around 3 K. Water was degassed several times before deposition. The matrices were generated by co-deposition of **5** and 0.5% of water with a large excess of argon (Messer Griesheim, 99.99%) on top of different substrates (Cu rod, CsI and sapphire windows respectively for EPR, FT-IR and UV-Vis spectroscopy) cooled at 3 K. A flow rate of approximately 1.80 sccm was used for the deposition of the matrix. T-**6** was generated by photolysis of **5** at 3 K using λ = 365 nm LED source. After annealing at 25 K for 10 minutes the matrices were cooled back to 3K. The experiments in LDA ice matrix were performed in the same manner but replacing the argon with water as explained above. FTIR spectra were recorded in the range between 400 and 4000 cm^{-1} with 0.5 cm^{-1} resolution. Matrix EPR spectra were recorded with a Bruker ELEXSYS 500 X-band spectrometer. Matrix UV-Vis spectra were recorded with a Varian Cary 5000 UV-Vis-NIR spectrophotometer in the range of 200 – 800 nm with a resolution of 0.1 nm.

Computational Methods

All gas-phase DFT geometry optimizations and frequency calculations were carried out using the B3LYP functional[3] with D3 empirical dispersion correction[4] and the def2-TZVP basis set. The TURBOMOLE program (version 6.4)[5] was employed. CCSD(T) single point calculations were performed using the cc-pVDZ basis set[6]. The MOLPRO program[7-8] was used for these calculations.

QM MD, QM/MM MD simulations and QM/MM optimizations were performed using the program ChemShell[9-10] as an interface to TURBOMOLE (version 6.4) and CHARMM 31b1.[11] QM MD simulations were conducted at the B3LYP-D3/def2-SVP level of theory while QM/MM MD simulations were carried out at the B3LYP-D3/def2-SVP//CHARMM level. These 10 ps MD simulations were performed with a time step of 2 fs under NVT (canonical) conditions at a temperature of 25 K. A Nosé–Hoover chain (NHC) thermostat[12-13] was used together with a reversible non-iterative leapfrog-type integrator. For the QM/MM MD simulations, the molecules of the QM regions (see below) were placed in boxes of water with a 15 Å padding. During the simulations the water molecules beyond 10 Å of the QM region were kept frozen. Before the QM/MM MD production runs, the QM atoms were kept frozen while the surrounding MM molecules were equilibrated for 5 ns under NPT conditions.

A total of 6 QM MD and QM/MM MD simulations of the following systems were performed: (1) QM MD: S-**FY**…$6H_2O$ and T-**FY** … $6H_2O$ in the gas phase; (2) QM/MM MD: S-**FY**…H_2O and T-**FY**…H_2O in a box of water; and (3) QM/MM MD: S-**FY**…$6H_2O$ and T-**FY**…$6H_2O$ in a box of water.

Additional QM/MM optimizations were performed on the following systems immersed in water boxes: (1) **FYH$^+$**…$^-$OH…$5H_2O$; (2) **FYH$^+$**…$6H_2O$; and (3) **FYH$^+$**…$12H_2O$.

QM MD and QM/MM MD simulations

a) QM/MM simulations of 1:1 FY-H_2O complexes in water

A 10 ps QM/MM MD simulation was run placing the 1:1 **FY**-water complexes in a box of water at 25 K. At B3LYP-D3/def2-SVP//CHARMM level of theory, neither the singlet nor the triplet complex showed evidence of thermal reaction in this timescale. To further asses the singlet-triplet splitting, 10 snapshots were taken from the trajectories and optimized at the B3LYP-D3/def2-TZVP//CHARMM level of theory (Table S5). In the case of the singlet complex the hydrogen bond is maintained throughout the simulation. In the case of the triplet complex, the geometry of the hydrogen bond is lost, suggesting that the water molecule prefer association with the surrounding waters, rather than to maintain the interaction with the carbene center. This leads to a further stabilization of the singlet complex over the triplet one making the singlet-triplet gap more negative (-4.5 ± 0.6 kcal/mol)

b) Simulations of the FY + 6H_2O systems in the gas phase

Gas phase QM MD simulations were carried out at 25K for 10ps. The level of theory used was B3LYP-D3/def2-SVP. Neither the singlet nor the triplet system underwent thermal reaction in these conditions. Like in the case of **FY**…H_2O in water, the hydrogen bond remains formed in the singlet complex while disappears in the triplet system. This is in contrast with the DPC…H_2O system, in which proton transfer from the water molecule to the carbene center was readily observed.

10 snapshots were taken from the trajectories and optimized at the B3LYP-D3/def2-TZVP level of theory (Table S6).

c) QM/MM simulations of the FY + 6H2O systems in a box of water

The previously described system was placed in a box of explicit water and used as QM region in 10 ps-long QM/MM MD simulations at the B3LYP-D3/def2-SVP//CHARMM level of theory. No evidence of thermal reaction was found in these simulations. The singlet system was allowed to run for an additional 10 ps, and still proton transfer was not observed. These findings are contrast with our previous findings for **DPC** using the BLYP functional, with predicted rapid reaction.

Here like in the gas phase, the hydrogen bond to the carbene center seems to disappear along the simulation of the triplet complexes while being preserved in the more polar singlet complex. This is more acute for **FY** than it was for **DPC** indicating that the triplet state of the former has a lower affinity towards water molecules, a fact that should play a role in the bigger inversion of the singlet triplet gap of **FY** as compared to **DPC**.

Experiments in Argon Matrices

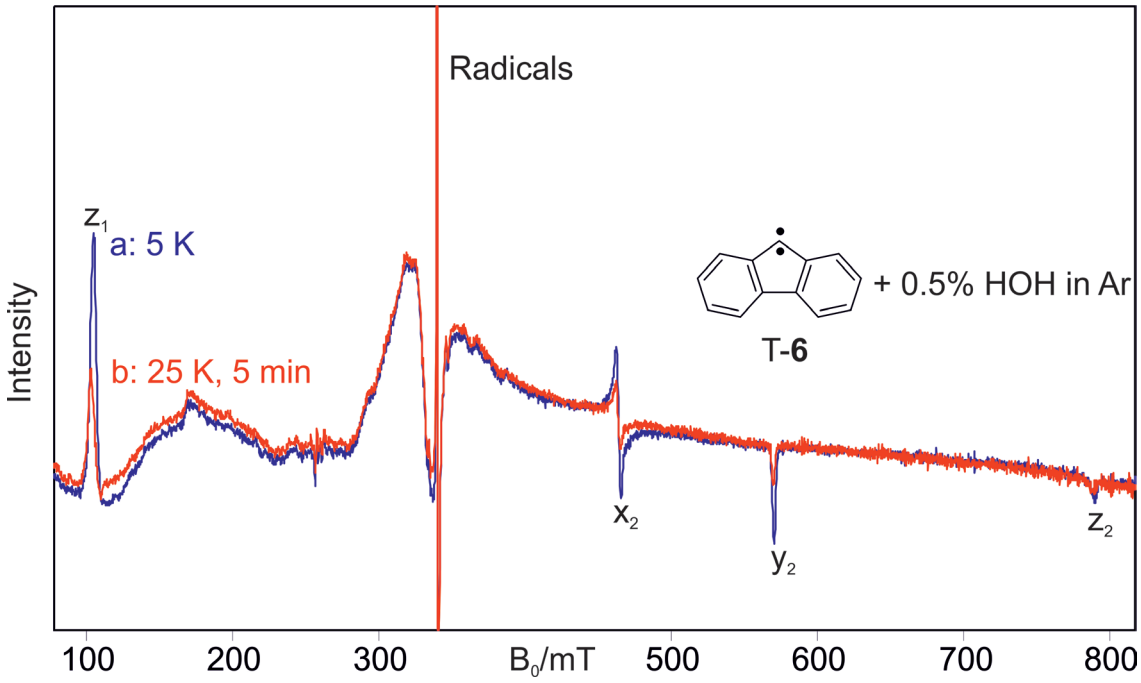

Figure S1. EPR spectra showing the reaction of T-6 in an argon matrix doped with 0.5 % water. a) Matrix at 5 K showing T-6 with the zfs parameters simulated D = 0.4215 cm^{-1}, E = 0.0265 cm^{-1}. b) After annealing for 5 min at 25 K, 59 % of the signal intensity of T-6 is lost. The radical signals are formed during the initial photolysis of the precursor and do not change in intensity during annealing.

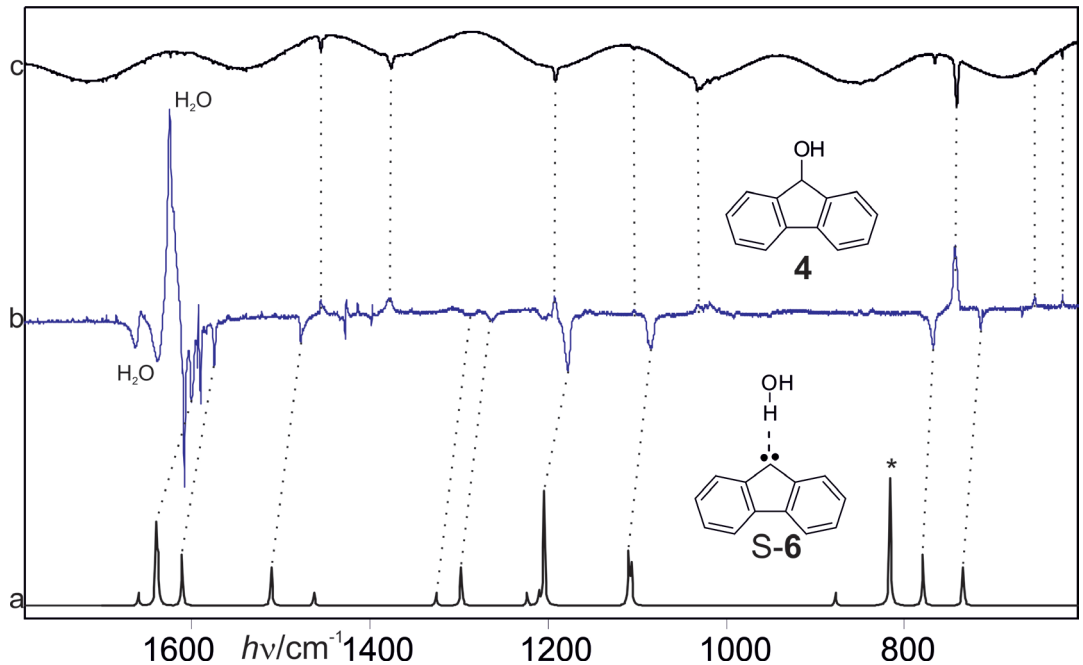

Figure S2. Difference IR spectra showing the disappearance of the complex S-6…HOH at 3 K after 14 h to form 9-Fluorenol (4). a) IR spectrum of the complex S-6...HOH calculated at the B3LYP-D3/def2-TZVP level of theory. b) Difference IR spectrum (Fig. 1-c). Bands pointing upwards are assigned to 4 are appearing and bands pointing downwards are assigned to S-6...HOH are disappearing. c) IR spectrum of 4 isolated in argon matrix at 3 K. *vibration of the O-H wagging.

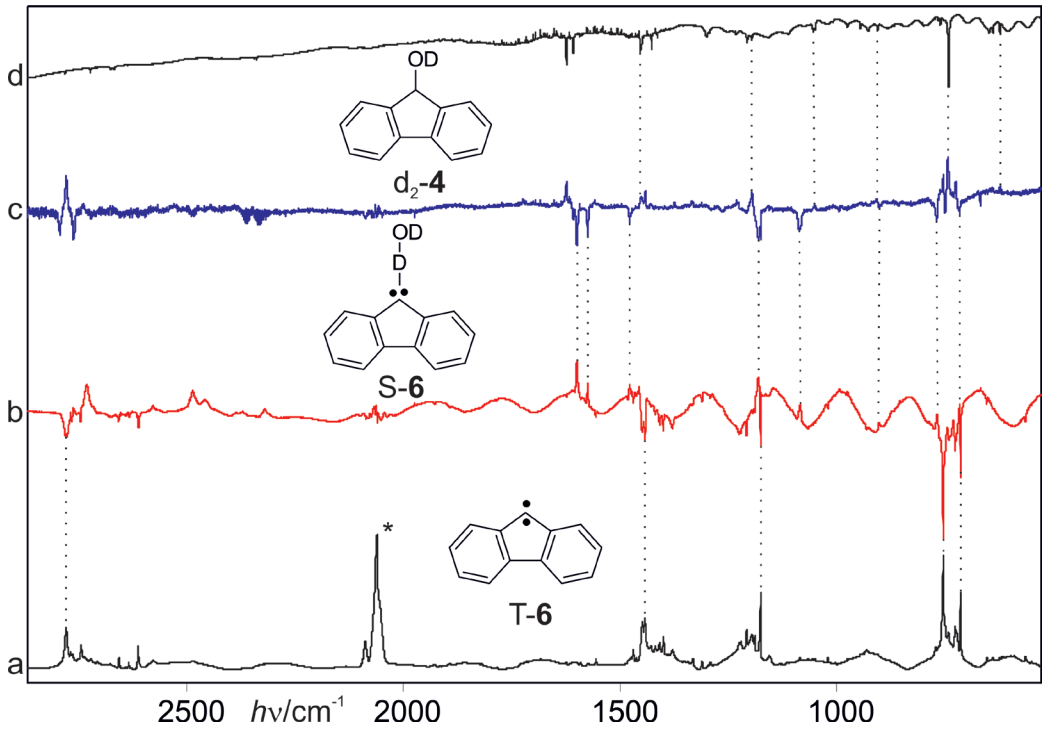

Figure S3. IR spectra showing the chemistry of fluorenylidene **6** in 0.5% D_2O-doped argon. a) T-**6** obtained after photolysis of **5** at 3 K. b) Difference IR spectrum of the same matrix after annealing for 10 min at 25 K. Bands pointing downwards assigned to T-**6** and D_2O are disappearing, bands pointing upwards assigned to the complex between S-**6** and D_2O are appearing. c) Difference IR spectrum after 14 hours at 3 K. Bands pointing upwards assigned to d_2-**4** are appearing, bands pointing downwards of S-1...D_2O are disappearing. d) d_2-**4** in argon at 3 K.

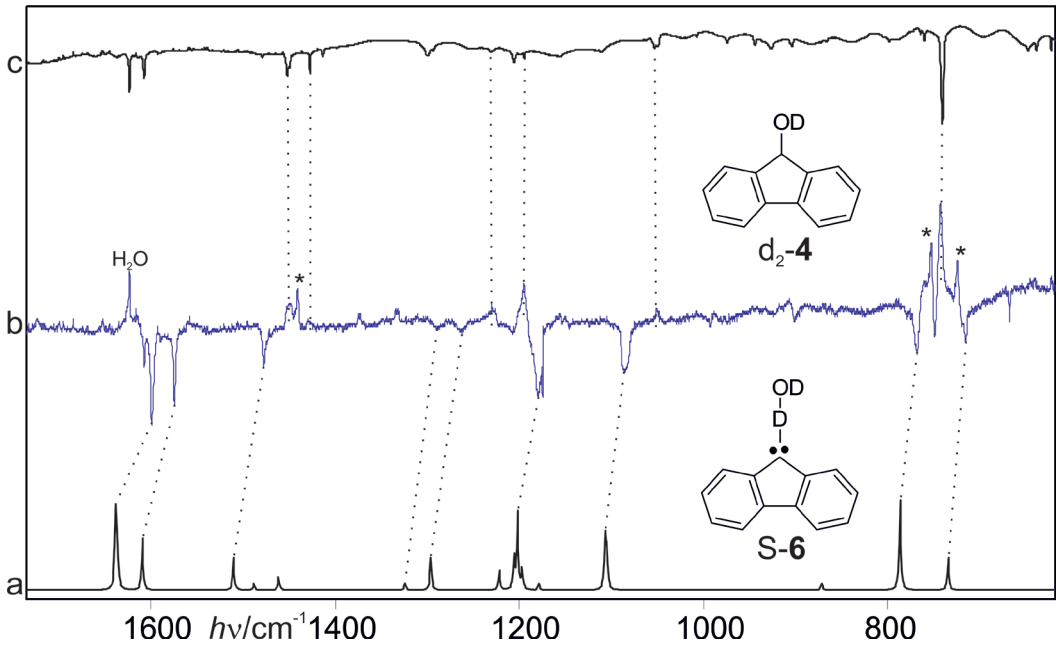

Figure S4. Difference IR spectra showing the disappearance of the complex S-6...DOD at 3 K after 14 h to form d_2-4. a) IR spectrum of the complex S-6...DOD calculated at the B3LYP-D3/ def2-TZVP level of theory. b) Difference IR spectrum (Fig. S3-c). Bands pointing upwards are assigned to d_2-4 are appearing and bands pointing downwards are assigned to S-6...DOD are disappearing. c) IR spectrum of d_2-4 isolated in argon matrix at 3 K. *signals caused by 9-Diazofluorene.

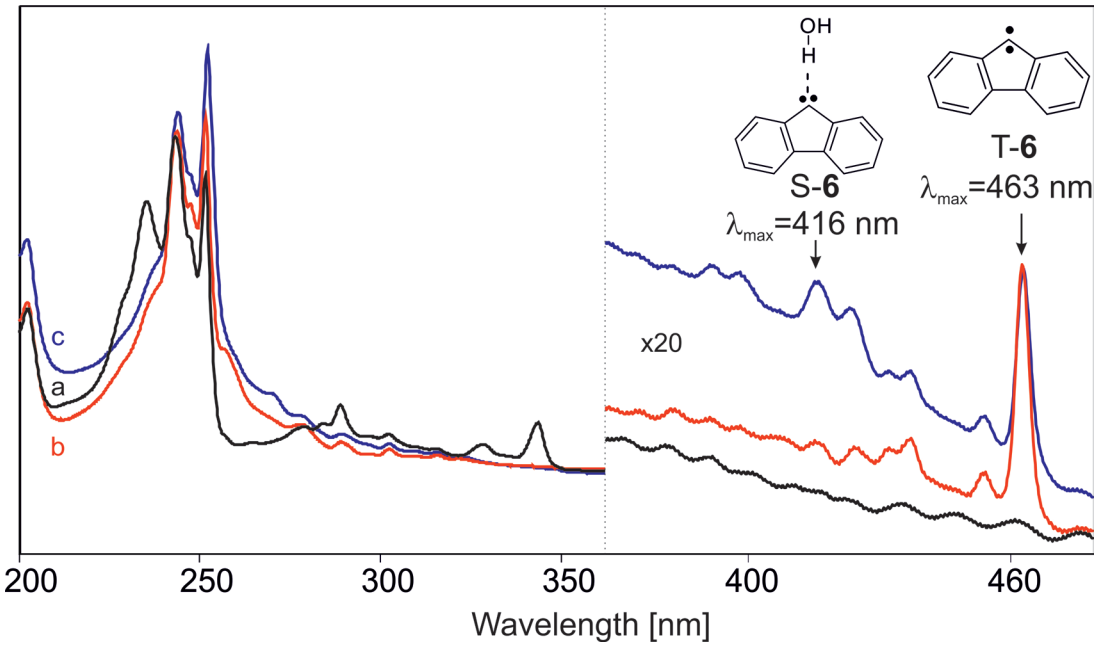

Figure S5. UV-vis spectra showing the photochemistry of **5** in argon doped with 0.5 % of water at 8 K. a) Deposition spectrum of **5**. b) 1 hour irradiation with λ = 365 nm. The band with λ_{max} 463 nm is assigned to T-**6**. c) 10 minutes annealing at 25 K. The band with λ_{max} = 416 nm is assigned to S-**6**...HOH, respectively.

Table S1. Reaction rate for the rearrangement of the complex between S-**6** and water to **4** at various temperatures. Reaction rate k is obtained by fitting the decrease of the integrated intensities of the signals to the equation: $y = g + a \exp(-kt)^c$.

T (K)	Species	g[a]	StdErr g	a	StdErr a	k (s-1)	StdErr k	c[b]	StdErr c
3	Complex S-6 + HOH	4.04E-01	4.67E-02	5.99E-01	4.78E-02	1.35E-05	2.44E-06	6.63E-01	2.03E-02
12	Complex S-6 + HOH	3.85E-01	5.06E-02	6.17E-01	5.16E-02	1.15E-05	2.34E-06	6.12E-01	1.86E-02
3	Complex S-6 + DOD	6.91E-01	6.62E-02	3.09E-01	6.68 E-02	6.78E-06	3.23E-06	6.52E-01	3.22E-02

[a]g = y intercept. [b]c = parameter for superposition of exponential decays.[14]

Table S2. IR spectroscopic data of the complex between S-**6** and H_2O.

S-**6**…HOH						
Mode	Sym	Calcd gas phase[a]		Argon[b]		
		ν/cm^{-1}	I_{rel}	ν/ cm^{-1}	I_{rel}	Assignment
20	A	734.4	38	714.6	72.2	C-H def. (o.o.p.)
23	A	779.3	53	767.8	100	C-H def.(o.o.p.)
37	A	1106.6	36	1084.4	50.0	C-H def. (i.p.)
41	A	1204.3	100	1178.0	77.8	C-C-C asym. str.
44	A	1297.1	28	1262.6	27.8	C-H def. (i.p.)
46	A	1325.1	12	1289.7	<27.8	C-H def. (i.p.)
51	A	1511.0	33	1477.9	33.3	C=C str. Ring
52	A	1610.6	50	1574.8	44.4	C=C str. Ring
55	A	1639.1	74	1600.4	66.7	C=C str. Ring

[a]Calculated at the B3LYP-D3/ def2-TZVP level of theory. [b]Argon matrix at 3 K.

Table S3. IR spectroscopic data of the complex between S-**6** and D_2O.

S-**6**…DOD								
Mode	Sym	Calcd gas phase[a]		Shift[b]	Argon[c]		Shift[b]	Assignment
		ν/cm^{-1}	I_{rel}		ν/ cm^{-1}	I_{rel}		
21	A	736.0	36	1.6	714.7	56.3	0.1	C-H def. (o.o.p.)
24	A	788.0	100	0.0	767.8	43.75	0.0	C-H def. (o.o.p.)
37	A	1106.0	43	-0.6	1086.4	31.3	2.2	C-H def. (i.p.)
41	A	1203.0	86	-1.3	1178.0	50.0	0.0	C-C-C asym str.
45	A	1297.1	36	0.0	1262.6	12.5	0.0	C-H def.(i.p.)
47	A	1325.1	7	0.0	1289.7	<12.5	0.0	C-H def.(i.p.)
52	A	1511.0	36	0.0	1478.0	25.0	0.1	C=C str. Ring
53	A	1610.6	57	0.0	1574.9	37.5	0.1	C=C str. Ring
56	A	1639.1	86	0.0	1599.6	100	-0.8	C=C str. Ring

[a]Calculated at the B3LYP-D3/ def2-TZVP level of theory. [b]Frequency shift relative to S-**1**…HOH. [c]Argon matrix at 3 K.

Experiments in water matrix

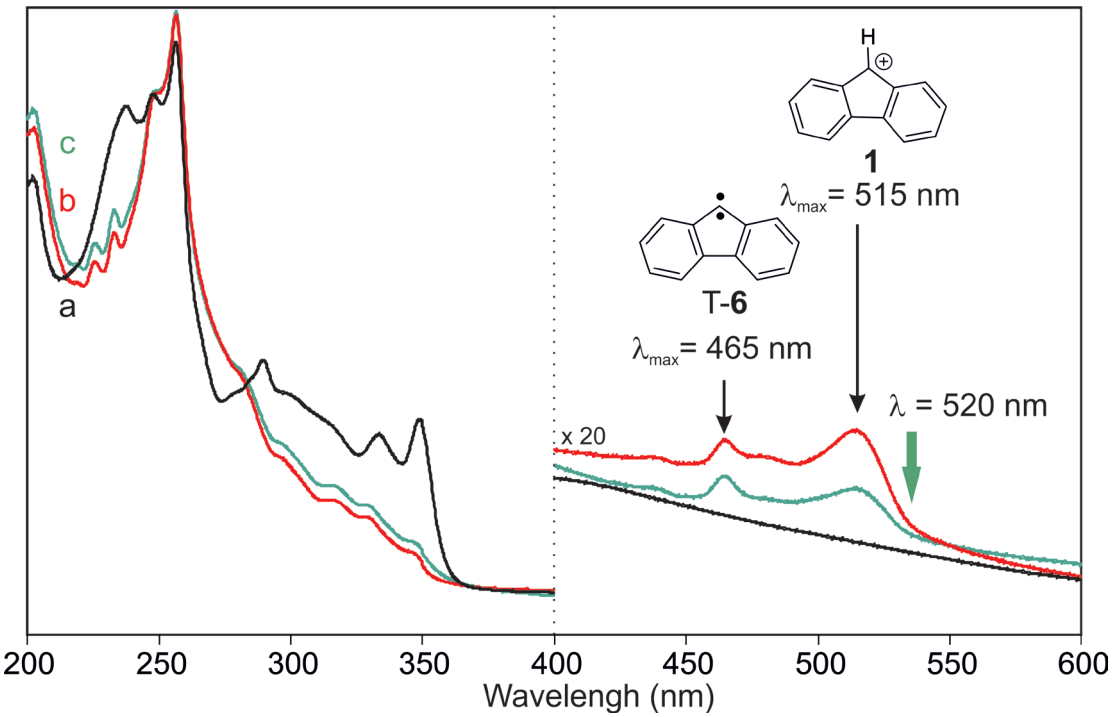

Figure S6. UV-vis spectra showing the photochemistry of **5** isolated in LDA ice at 8 K. a) Deposition spectrum of **5** in LDA ice. b) 10 minutes irradiation with λ = 365 nm. The bands with λ_{max} = 515 nm and λ_{max} = 465 nm are assigned to **1** and T-**6**. c) 10 minutes irradiation with λ = 520 nm. Band assigned to **1** decreases in intensity.

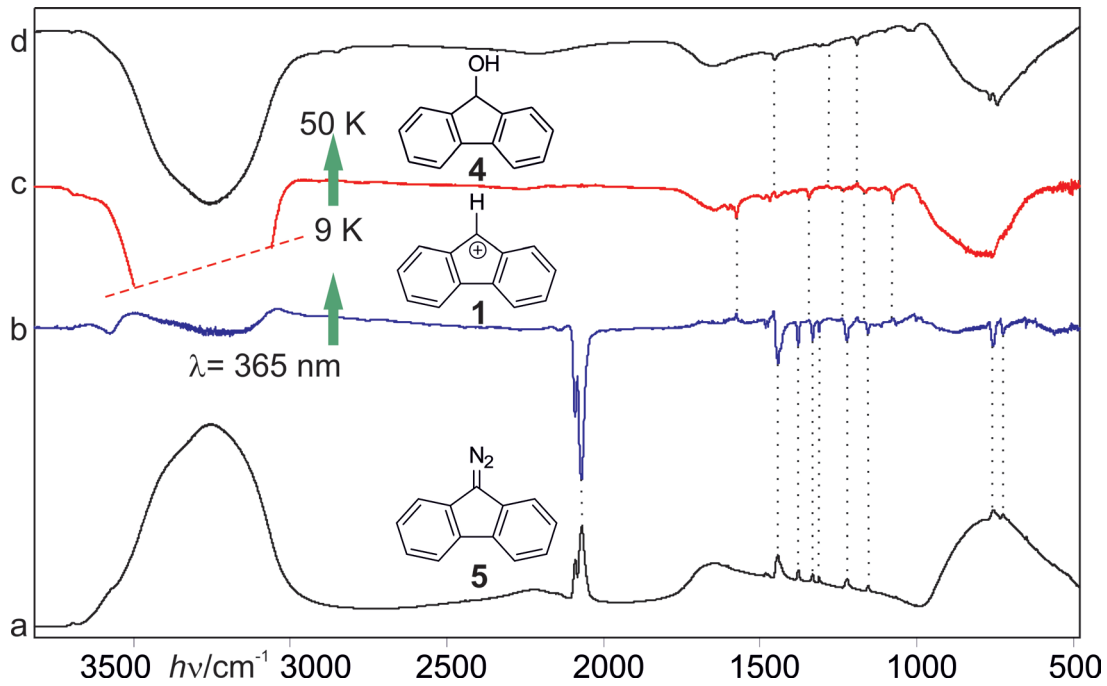

Figure S7. IR spectra showing the formation and reaction of the fluorenyl cation 1. a) 5 in LDA ice at 9 K. b) Difference IR spectrum of the same matrix after irradiation at 9 K showing the generation of 1. Bands pointing downwards assigned to 5 are disappearing and bands pointing upwards assigned to 4 and 1 are appearing. c) Difference IR spectrum of the same matrix after annealing at 50 K showing the formation of the O-H insertion product. Bands pointing upwards are assigned to 4 are appearing and bands pointing downwards are assigned to 1 are disappearing. d) deposition spectrum of 4 in LDA ice at 9 K.

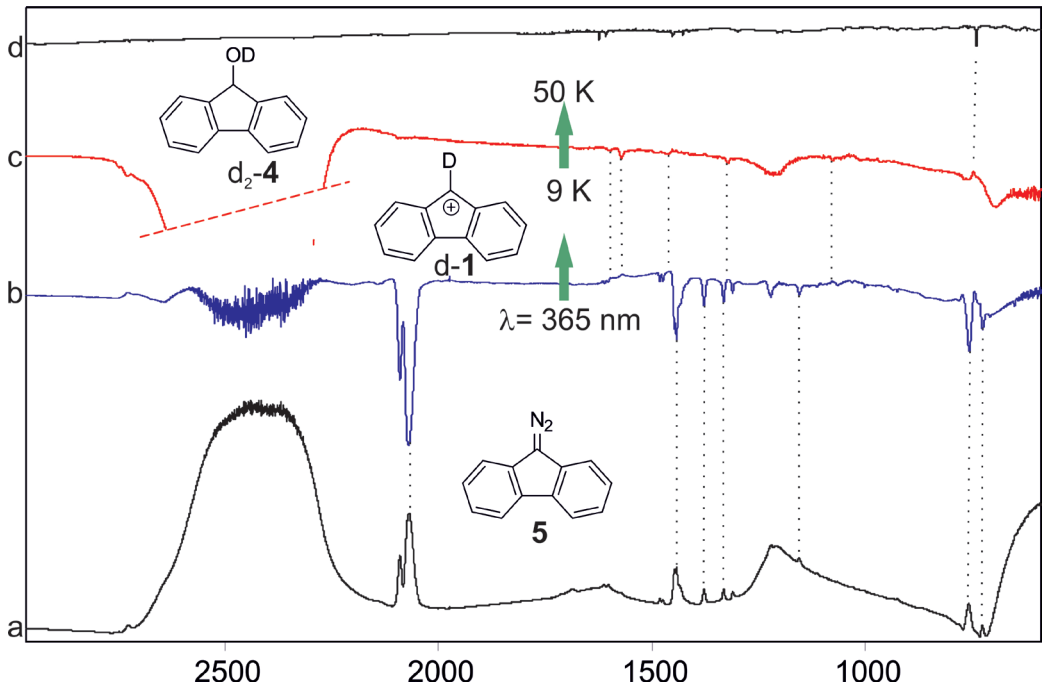

Figure S8. IR spectra showing the formation and reaction of the d-1. a) 5 in LDA ice at 50 K. b) Difference IR spectrum of the same matrix after irradiation at 9 K showing the generation of d-1. Bands pointing downwards assigned to 5 are disappearing and bands pointing upwards assigned to the O-D insertion product and d-1 are appearing. c) Difference IR spectrum of the same matrix after annealing at 50 K showing the formation of the O-D insertion product. Bands pointing upwards are assigned to d_2-4 are appearing and bands pointing downwards are assigned to d-1 are disappearing. d) deposition spectrum of d_2-4 in argon at 3 K.

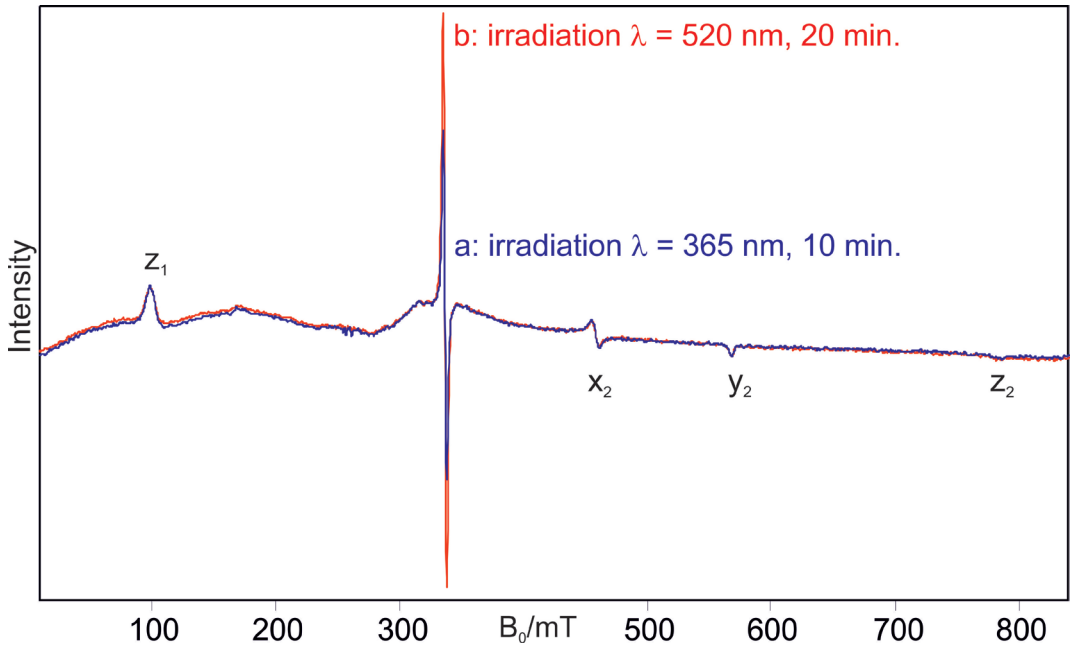

Figure S9. EPR spectra showing the reaction of 5 in LDA ice at 5 K. a) Matrix at 5 K showing T-6 after irradiation for 10 min at 365 nm. b) After irradiation for 20 min at 520 nm the radical signals increased. The triplet signals do not change in intensity during photolysis.

Computational details

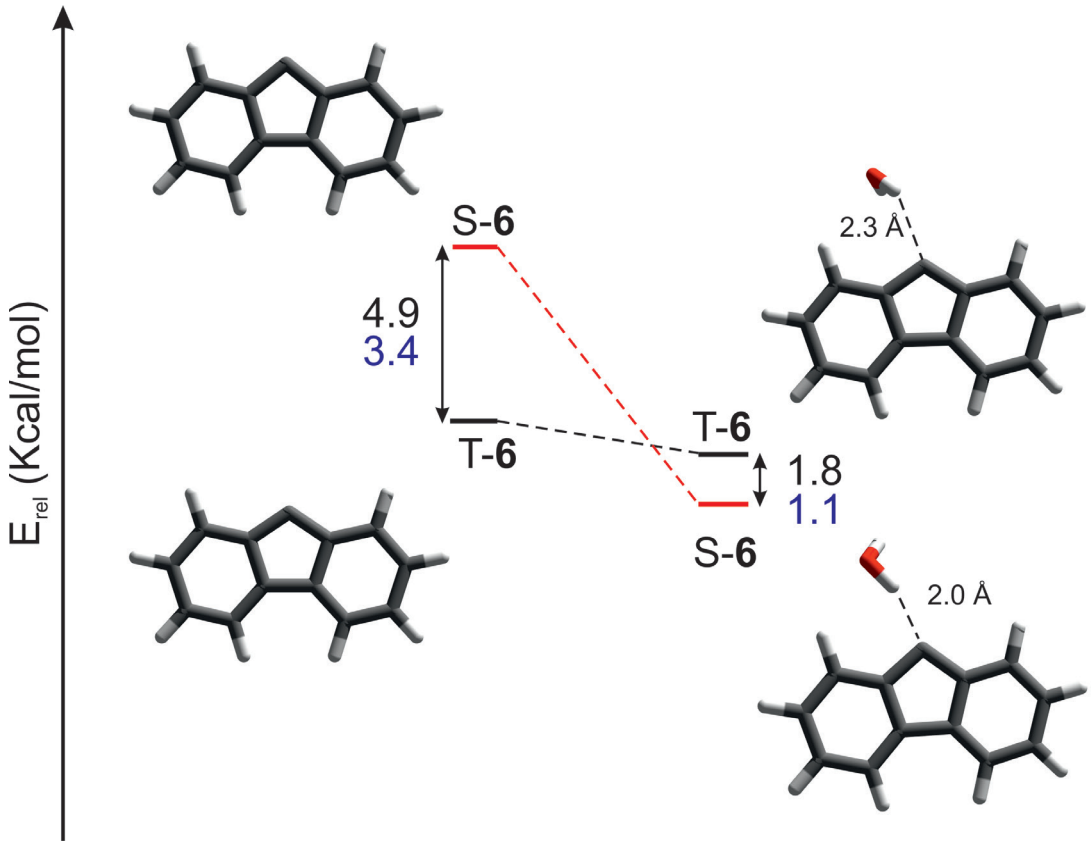

Figure S10. S-T gaps (kcal/mol) of **6** and its most stable complexes with water computed at the B3LYP-D3/def2-TZVP level of theory (singlet energies in red, triplet energies in black, all energies including ZPE correction). Values in blue correspond to the (CCSD(T)/cc-pVDZ//B3LYP-D3/def2-TZVP) level of theory.

Table S4. Singlet-triplet gap (kcal/mol) and selected geometrical parameters of **6** and it´s 1:1 water complexes at the B3LYP-D3/def2-TZVP level of theory.

	Θ(C-C-C)	Θ(C-H-O)	R(C-H) (Å)	ΔE (S-T)[a]	ΔE_{ZPE} (S-T)[b]
			FY		
S-**FY**	102°	-	-	4.9	4.9
T-**FY**	112°	-	-		
			Complexes		
S-**FY** … H_2O	103°	160°	1.96Å	-2.6	-1.8
T-**FY** … H_2O	113°	140°	2.30Å		

[a]Energies uncorrected by ZPE. [b]Energies corrected by ZPE

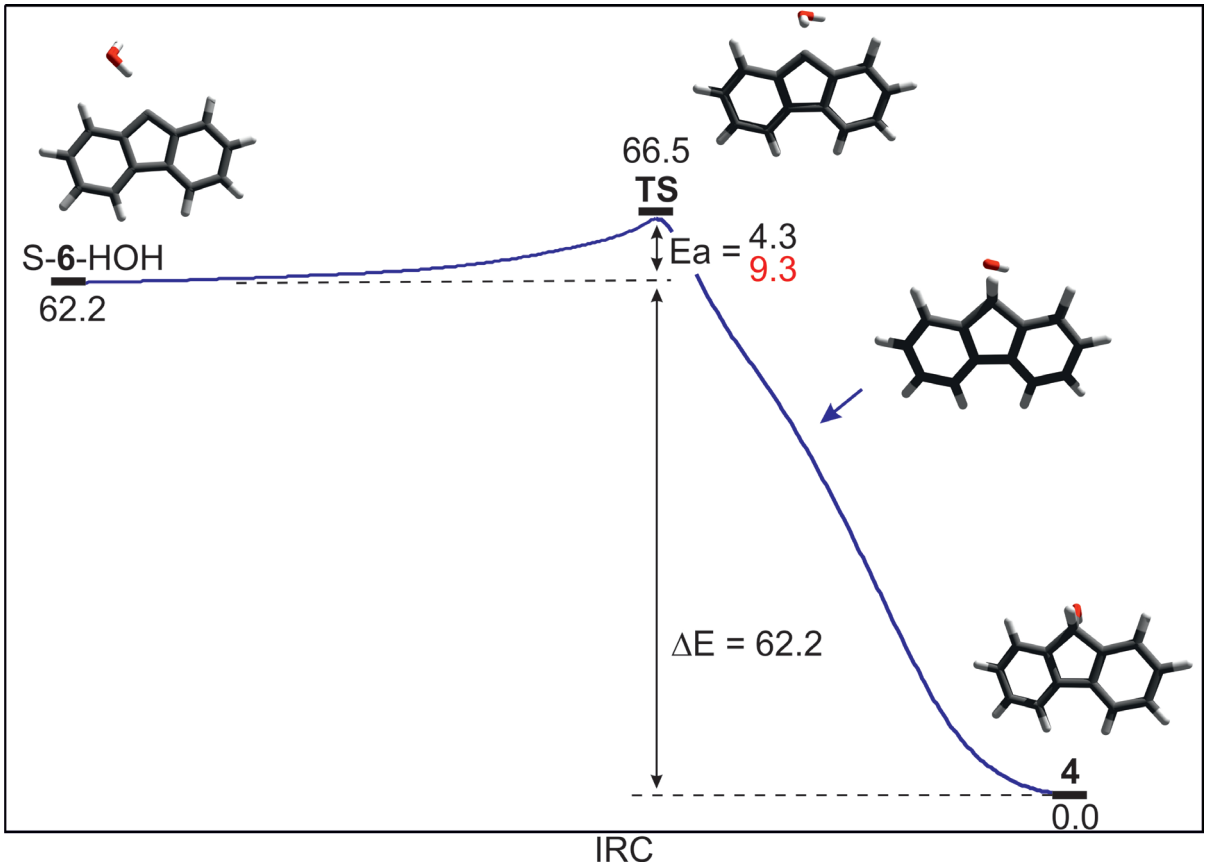

Figure S11. Intrinsic reaction coordinate (IRC) for the rearrangement of the complex S-**6** … H_2O to **4** calculated at the BLYP-D3/def2-TZVP level of theory. Energies are given in kcal/mol, the CCSD(T)/cc-pVTZ//BLYP-D3/def2-TZVP calculated activation barrier E_a is shown in red.

Table S5. Singlet-triplet gap (kcal/mol) and selected geometrical parameters of the 1:1 **FY**-water complexes at the B3LYP-D3/def2-TZVP//CHARMM level of theory

	Θ(C-C-C)		**R(C-H) (Å)**		**Θ(C-H-O)**		**ΔE_{ZPE} (S-T)**
	S-**FY**…H_2O	T-**FY**…H_2O	S- **FY**…H_2O	T- **FY**…H_2O	S- **FY**…H_2O	T- **FY**…H_2O	
1	103.1°	111.9°	1.97	2.66	156.8°	107.4°	-5.5
2	103.1°	111.9°	1.96	2.65	157.5°	102.7°	-4.7
3	103.1°	111.9°	1.97	2.66	157.7°	102.5°	-3.7
4	103.2°	111.8°	1.97	2.66	156.0°	96.3°	-5.2
5	103.2°	111.8°	1.97	2.66	155.6°	96.6°	-4.5
6	103.1°	111.9°	1.98	2.66	157.5°	97.2°	-3.4
7	103.3°	111.8°	1.94	2.64	156.2°	97.8°	-5.3
8	103.2°	111.8°	1.97	2.64	156.0°	97.4°	-4.6
9	103.1°	111.8°	1.98	2.60	158.4°	96.8°	-4.1
10	103.2°	111.8°	1.94	2.62	157.7°	95.3°	-4.1
Average	**103.16°**	**111.84°**	**1.97**	**2.65**	**156.9°**	**99°**	**-4.5**
MAE	**0.06**	**0.05**	**0.01**	**0.02**	**0.8**	**3**	**0.6**

Table S6. Singlet-triplet gap (kcal/mol) and selected geometrical parameters of the **FY**…$6H_2O$ systems at the B3LYP-D3/def2-TZVP level of theory

	Θ(C-C-C)		**R(C-H) (Å)**		**Θ(C-H-O)**		**ΔE_{ZPE} (S-T)**
	S-**FY**…H_2O	T-**FY**…H_2O	S- **FY**…H_2O	T- **FY**…H_2O	S- **FY**…H_2O	T- **FY**…H_2O	
1	103.2°	112.1°	1.80	3.21	169.4°	88.4°	-0.6
2	103.2°	112.1°	1.81	3.22	169.6°	88.0°	-0.5
3	103.0°	112.1°	1.85	3.21	164.0°	88.8°	-0.5
4	103.0°	112.0°	1.85	3.24	164.2°	93.4°	-0.6
5	103.2°	112.1°	1.81	3.21	169.3°	88.4°	-0.6
6	103.2°	112.1°	1.81	3.21	169.4°	88.8°	-0.6
7	103.1°	112.2°	1.81	3.22	169.2°	88.4°	-0.6
8	103.2°	112.1°	1.81	3.22	169.4°	88.2°	-0.6
9	103.2°	112.2°	1.81	3.22	169.3°	88.0°	-0.5
10	103.2°	112.0°	1.81	3.21	169.3°	88.2°	-0.6
Average	**103.15°**	**112.10°**	**1.82**	**3.217**	**168.3°**	**88.9°**	**-0.57**
MAE	**0.07**	**0.04**	**0.02**	**0.007**	**1.7**	**0.9**	**0.04**

Table S7. Cartesian coordinates of the optimized structure of S-6 calculated at the B3LYP-D3/def2-TZVP level of theory

Atomic Symbol	x	y	z
C	0.000	3.032	-1.110
C	0.000	3.438	0.217
C	0.000	2.485	1.243
C	0.000	1.137	0.915
C	0.000	0.739	-0.449
C	0.000	1.668	-1.461
H	0.000	3.779	-1.895
H	0.000	4.494	0.455
H	0.000	2.781	2.285
H	0.000	1.376	-2.505
C	0.000	0.000	1.843
C	0.000	-1.137	0.915
C	0.000	-2.485	1.243
C	0.000	-3.438	0.217
C	0.000	-3.032	-1.110
C	0.000	-1.668	-1.461
C	0.000	-0.739	-0.449
H	0.000	-2.781	2.285
H	0.000	-4.494	0.455
H	0.000	-3.779	-1.895
H	0.000	-1.376	-2.505
E = -500.2801608, ZPE = 0.1625686, Ec = -500.1175922			
E = -498.6727291 (CCSD(T)/cc-pVDZ// B3LYP-D3/def2-TZVP)			

Table S8. Cartesian coordinates of the optimized structure of T-**6** calculated at the B3LYP-D3/def2- TZVP level of theory

Atomic Symbol	x	y	z
C	0.000	3.022	-1.127
C	0.000	3.453	0.201
C	0.000	2.539	1.249
C	0.000	1.175	0.949
C	0.000	0.733	-0.416
C	0.000	1.660	-1.441
H	0.000	3.753	-1.925
H	0.000	4.514	0.417
H	0.000	2.874	2.278
H	0.000	1.339	-2.476
C	0.000	0.000	1.740
C	0.000	-1.175	0.949
C	0.000	-2.539	1.249
C	0.000	-3.453	0.201
C	0.000	-3.022	-1.127
C	0.000	-1.660	-1.441
C	0.000	-0.733	-0.416
H	0.000	-2.874	2.278
H	0.000	-4.514	0.417
H	0.000	-3.753	-1.925
H	0.000	-1.339	-2.476
E = -500.2879699, ZPE = 0.1626441, Ec = -500.1253258			
E = -498.6781185 (CCSD(T)/cc-pVDZ// B3LYP-D3/def2- TZVP)			

Table S9. Cartesian coordinates of the optimized structure of **1** calculated at the B3LYP-D3/def2- TZVP level of theory

Atomic Symbol	x	y	z
C	-3.045	-1.121	0.000
C	-3.456	0.205	0.000
C	-2.509	1.229	0.000
C	-1.156	0.876	0.000
C	-0.742	-0.490	0.000
C	-1.675	-1.487	0.000
H	-3.792	-1.905	0.000
H	-4.511	0.442	0.000
H	-2.812	2.268	0.000
H	-1.397	-2.533	0.000
C	0.000	1.691	0.000
C	1.156	0.876	0.000
C	2.509	1.229	0.000
C	3.456	0.205	0.000
C	3.045	-1.121	0.000
C	1.675	-1.487	0.000
C	0.742	-0.490	0.000
H	2.812	2.268	0.000
H	4.511	0.442	0.000
H	3.792	-1.905	0.000
H	1.397	-2.533	0.000
H	0.000	2.774	0.000
E = -500.7289432, ZPE = 0.1765799, Ec = -500.5523633			

Table S10. Cartesian coordinates of the optimized structure of S-**6…**H_2O calculated at the B3LYP-D3/def2-TZVP level of theory

Atomic Symbol	x	y	z
C	2.425	-2.220	-0.003
C	3.143	-1.033	0.010
C	2.473	0.198	0.020
C	1.083	0.199	0.016
C	0.361	-1.026	0.002
C	1.015	-2.232	-0.007
H	2.958	-3.163	-0.011
H	4.225	-1.060	0.011
H	3.005	1.141	0.030
H	0.480	-3.174	-0.018
C	0.205	1.363	0.021
C	-1.125	0.759	0.012
C	-2.350	1.411	0.011
C	-3.526	0.651	0.000
C	-3.459	-0.735	-0.011
C	-2.223	-1.412	-0.011
C	-1.073	-0.662	0.001
H	-2.382	2.493	0.018
H	-4.491	1.141	-0.001
H	-4.376	-1.312	-0.020
H	-2.198	-2.495	-0.021
O	2.206	3.468	-0.100
H	1.381	2.923	-0.058
H	2.063	4.197	0.509
E = -576.7623041, ZPE = 0.1869368, Ec = -576.5753673			
E = -574.9304948 (CCSD(T)/cc-pVDZ// B3LYP-D3/def2-TZVP)			

Table S11. Cartesian coordinates of the optimized structure of T-**6…**H_2O calculated at the B3LYP-D3/def2-TZVP level of theory

Atomic Symbol	x	y	z
C	2.396	-2.251	0.015
C	3.144	-1.073	-0.022
C	2.521	0.170	-0.046
C	1.126	0.214	-0.034
C	0.354	-0.996	0.002
C	0.998	-2.218	0.027
H	2.906	-3.206	0.033
H	4.225	-1.128	-0.033
H	3.091	1.089	-0.078
H	0.431	-3.141	0.054
C	0.180	1.268	-0.049
C	-1.156	0.801	-0.028
C	-2.401	1.431	-0.034
C	-3.547	0.645	-0.007
C	-3.459	-0.749	0.027
C	-2.218	-1.392	0.033
C	-1.065	-0.631	0.005
H	-2.471	2.511	-0.061
H	-4.521	1.117	-0.011
H	-4.366	-1.340	0.048
H	-2.165	-2.474	0.059
O	2.255	3.574	0.009
H	1.488	3.131	-0.380
H	2.095	3.532	0.958
E = -576.7581259, ZPE = 0.1855976, Ec = -576.5725283			
E = -574.9288058 (CCSD(T)/cc-pVDZ// B3LYP-D3/def2-TZVP)			

Table S12. Cartesian coordinates of the optimized structure of **TS** calculated at the B3LYP-D3/def2- TZVP level of theory

Atomic Symbol	x	y	z
C	3.023	-1.464	0.160
C	3.439	-0.154	-0.058
C	2.503	0.856	-0.285
C	1.154	0.533	-0.265
C	0.737	-0.798	-0.011
C	1.662	-1.802	0.179
H	3.764	-2.238	0.319
H	4.496	0.079	-0.058
H	2.813	1.879	-0.459
H	1.357	-2.828	0.348
C	0.004	1.374	-0.556
C	-1.152	0.536	-0.260
C	-2.502	0.858	-0.293
C	-3.442	-0.149	-0.064
C	-3.027	-1.458	0.161
C	-1.667	-1.797	0.183
C	-0.738	-0.796	-0.007
H	-2.817	1.875	-0.493
H	-4.499	0.084	-0.075
H	-3.769	-2.231	0.319
H	-1.364	-2.824	0.350
O	0.102	3.237	0.707
H	0.017	2.679	-0.312
H	-0.781	3.200	1.099
E = -576.7514645, ZPE = 0,1829554, Ec = -576.5685091 E = -574.9156951 (CCSD(T)/cc-pVDZ// B3LYP-D3/def2- TZVP)			

Table S13. Cartesian coordinates of the optimized structure of **4** calculated at the B3LYP-D3/def2- TZVP level of theory

Atomic Symbol	x	y	z
C	3.008	-1.435	0.097
C	3.448	-0.118	-0.029
C	2.530	0.924	-0.173
C	1.181	0.623	-0.181
C	0.735	-0.699	-0.040
C	1.648	-1.737	0.093
H	3.733	-2.232	0.203
H	4.509	0.096	-0.017
H	2.866	1.949	-0.269
H	1.314	-2.762	0.197
C	0.000	1.566	-0.331
C	-1.181	0.623	-0.181
C	-2.530	0.924	-0.173
C	-3.448	-0.118	-0.029
C	-3.008	-1.435	0.097
C	-1.648	-1.737	0.093
C	-0.735	-0.699	-0.040
H	-2.866	1.949	-0.269
H	-4.509	0.096	-0.017
H	-3.733	-2.232	0.203
H	-1.314	-2.762	0.197
O	0.000	2.682	0.555
H	0.000	2.013	-1.330
H	0.000	2.344	1.459
E = -576.8665859, ZPE = 0.1920717, Ec = -576.6745142 E = -575.0424521 (CCSD(T)/cc-pVDZ// B3LYP-D3/def2- TZVP)			

References

[1] W. Zeng, T. Eric Ballard, A. G. Tkachenko, V. A. Burns, D. L. Feldheim, C. Melander, *Bioorganic & Medicinal Chemistry Letters* **2006**, *16*, 5148-5151.

[2] A. R. Brown, W.-H. Kuo, E. N. Jacobsen, *Journal of the American Chemical Society* **2010**, *132*, 9286-9288.

[3] A. D. Becke, *The Journal of Chemical Physics* **1993**, *98*, 5648-5652.

[4] S. Grimme, J. Antony, S. Ehrlich, H. Krieg, *The Journal of Chemical Physics* **2010**, *132*, -.

[5] R. Ahlrichs, M. Bär, M. Häser, H. Horn, C. Kölmel, *Chem. Phys. Lett.* **1989**, *162*, 165-169.

[6] T. H. Dunning, *The Journal of Chemical Physics* **1989**, *90*, 1007-1023.

[7] H.-J. Werner, P. J. Knowles, G. Knizia, F. R. Manby, M. Schütz, *Wiley Interdisciplinary Reviews: Computational Molecular Science* **2012**, *2*, 242-253.

[8] Chemshell, a Computational Chemistry Shell

[9] P. Sherwood, A. H. de Vries, M. F. Guest, G. Schreckenbach, C. R. A. Catlow, S. A. French, A. A. Sokol, S. T. Bromley, W. Thiel, A. J. Turner, S. Billeter, F. Terstegen, S. Thiel, J. Kendrick, S. C. Rogers, J. Casci, M. Watson, F. King, E. Karlsen, M. Sjøvoll, A. Fahmi, A. Schäfer, C. Lennartz, *Journal of Molecular Structure: THEOCHEM* **2003**, *632*, 1-28.

[10] G. Maier, N. H. Wiegand, S. Baum, R. Wuellner, *Chem. Ber.* **1989**, *122*, 781-794.

[11] B. R. Brooks, C. L. Brooks, A. D. Mackerell, L. Nilsson, R. J. Petrella, B. Roux, Y. Won, G. Archontis, C. Bartels, S. Boresch, A. Caflisch, L. Caves, Q. Cui, A. R. Dinner, M. Feig, S. Fischer, J. Gao, M. Hodoscek, W. Im, K. Kuczera, T. Lazaridis, J. Ma, V. Ovchinnikov, E. Paci, R. W. Pastor, C. B. Post, J. Z. Pu, M. Schaefer, B. Tidor, R. M. Venable, H. L. Woodcock, X. Wu, W. Yang, D. M. York, M. Karplus, *J. Comput. Chem.* **2009**, *30*, 1545-1614.

[12] S. Nosé, *The Journal of Chemical Physics* **1984**, *81*, 511-519.

[13] W. G. Hoover, *Physical Review A* **1985**, *31*, 1695-1697.

[14] W. Sander, G. Bucher, F. Reichel, D. Cremer, *Journal of the American Chemical Society* **1991**, *113*, 5311-5322.